JOURNAL OF Materials CHEMISTRY

Discotic liquid crystals of transition metal complexes. Part 24† Synthesis and mesomorphism of porphyrin derivatives substituted with two or four bulky groups

Kazuchika Ohta,* Noboru Yamaguchi and Iwao Yamamoto

Department of Functional Polymer Science, Faculty of Textile Science and Technology, Shinshu University, 386–8567 Ueda, Japan. E-mail: ko52517@giptc.shinshu-u.ac.jp

Received 21st July 1998, Accepted 2nd September 1998

We have synthesized nine novel porphyrin derivatives, **1**–**8** and **1-Cu**, substituted with various steric hindrance groups and long flexible chains in order to investigate the relationship between the molecular type of porphyrin derivatives and the resulting mesophase. Type 4 disc-like $(C_{12}O)_{16}$-TTPH$_2$ (**1**) and $(C_{12}O)_{16}$-TTPCu (**1-Cu**) derivatives exhibit D_h columnar mesophases, which are the first examples of *meso*-substituted porphyrin metal-free derivatives and copper complexes. Type 5 strip-like $(C_nO)_8$-BTPH$_2$ [**4** ($n=12$), **5** ($n=16$)] derivatives having eight long chains at the 5,15-positions exhibit D_{rd} columnar mesophases. On the other hand, the type 5 $(C_{12}O)_4$-BTPH$_2$ (**6**) derivative having four long chains exhibits discotic lamellar $D_{L.rec1}$ and $D_{L.rec2}$ mesophases which have a two-dimensional rectangular structure within the layer. The $(C_{12}O)_4$-BPPH$_2$ (**7**) type 6 derivative also shows a D_L lamellar mesophase. Bruce *et al.* reported that type 3 rod-like porphyrin derivatives show calamitic mesophases of S_B, S_E and $S_{E'}$ phases. We revealed from these types of mesogenic porphyrin derivatives that such a successive change of the molecular structures causes their mesophases to change from discotic columnar to discotic lamellar, and further to calamitic.

1. Introduction

Porphyrins and their analogues exist in various states in nature and act as centers of energy transfer and charge transfer processes. In order to reveal their mechanistic role in natural systems, a number of porphyrin derivatives have been synthesized and studied extensively as models of vital functions.[2,3] Moreover, porphyrins are expected to find applications in functional materials because of their favorable electronic properties, chemical and thermal stabilities.

For the effective utilization of functionalities of a certain molecule, it is important to control the electronic and steric environments and the state of aggregation of the molecules. For this purpose, the following methods have been used: (a) enlargement of the π-conjugated system,[4] (b) giving molecular recognizability by modification of the molecule with bulky substituent,[3] and (c) formation of aggregates such as membranes, micelles, or microemulsions by introduction of aliphatic, hydrophilic, or amphiphilic substituents.[5] It may be very useful to incorporate liquid crystallinity to organic metal complexes with various valuable characteristics, in order to provide new properties or to modify known properties of the original complexes. For example, it was reported that the third-order nonlinear optical susceptibility ($\chi^{(3)}$) of tetrakis-(octylthio)phthalocyaninatocopper(II) in the mesomorphic state is larger than that in the solid state.[6]

The first study of mesogenic porphyrins was reported in 1980 for uroporphyrin I octa-*n*-dodecyl ester which shows a monotropic discotic mesophase.[7] Since then, some mesogenic porphyrins have been synthesized and their mesomorphic properties investigated,[8–17] although there are fewer mesogenic porphyrins than mesogenic phthalocyanines[18] whose core shape is very analogous to porphyrin. Most of the mesogenic porphyrins have been synthesized mainly from the photophysical viewpoint.

Liquid crystals containing the porphyrin core reported to date can be classified into three types by means of their molecular shapes (see Fig. 1). Type 1 consists of the β-

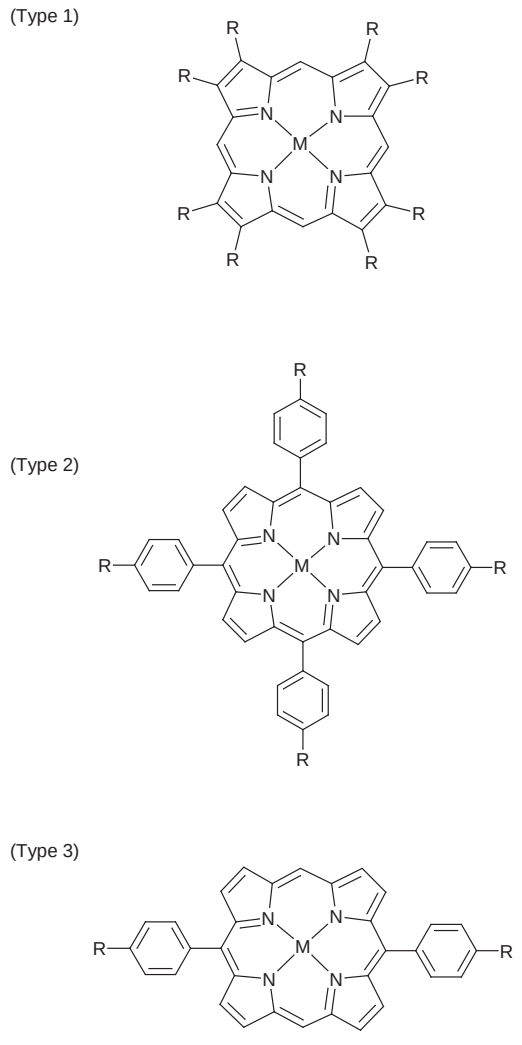

Fig. 1 Three types of mesogenic porphyrin derivatives reported to date.

†Part 23: Ref. 1.

substituted porphyrin derivatives. Greg *et al.* synthesized many octakis-substituted porphyrin derivatives which exhibit a discotic columnar mesophase.[8,9] Octakis(alkoxyethyl)porphyrinatozinc(II) was investigated in terms of the photovoltaic effect[9] and radiation-induced conductivity.[10] It was reported by Doppelt[11] and Morelli *et al.*[12] that octakis(octylthio)tetraazaporphyrin metal complexes show a discotic hexagonal columnar (D_h) mesophase. The compounds of this type tend to form a columnar mesophase in which the molecules stack one-dimensionally because of the flatness of the molecule. Type 2 is the *meso*-substituted porphyrin derivatives. Shimizu *et al.* synthesized a series of tetra-(long-alkyl chain)-substituted tetraphenylporphyrins and reported that they exhibit a discotic lamellar (D_L) mesophase.[13] They characterized several properties such as photoconductivity,[14] third-order nonlinear optical susceptibility,[15] and so on. Besides, some long chain esters of *meso*-tetrakis(*p*-carboxyphenyl)porphyrin were reported to exhibit an identified phase with a lamellar structure.[16] From these examples mentioned above, compounds of type 2 show not a columnar mesophase but a lamellar mesophase because van der Waals interaction between the porphyrin macrocycles have been weakened by the existence of bulky groups (phenyl groups) near the porphyrin core, and because the small number of flexible chains around the core are not enough to occupy all the surrounding area to form a columnar structure.

On the other hand, it was reported by Bruce *et al.* that 5,15-bis(*p*-alkoxyphenyl)porphyrinatozinc(II), belonging to type 3, shows smectic B, E, and E′ phases (abbreviated as S_B, S_E and $S_{E'}$, respectively).[17] It is interesting that this porphyrin, the molecular shape of which is basically discotic (disk-like), shows not discotic columnar mesophases but calamitic mesophases, although long-chain-substituted disk-like compounds generally tend to show columnar mesophases.

We noticed that the porphyrin derivatives could more easily change their molecular shapes compared with other macrocyclic compounds such as phthalocyanines. From this synthetic viewpoint, a great variety of mesogenic porphyrin derivatives will be able to be obtained. In order to study how the mesomorphism may change with changing the kind of bulky group and/or the number of flexible long alkyl chains in the surroundings of a porpyrin core, we have synthesized nine novel porphyrin derivatives of four types, **1**–**8** and **1-Cu**, as illustrated in Fig. 2, and investigated their mesomorphism.

Compounds **1**–**3** have four *o*-terphenyl groups with long alkoxy chains at the 5, 10, 15 and 20-positions of the porphyrin, and they are abbreviated as $(C_nO)_m$-TTPM ($n=8$, 12; $m=8$, 16; M = H_2, Cu). Compounds **4**–**6** have two of the *o*-terphenyl groups replaced by two *o*-terphenyl groups with long alkoxy chains at the 5 and 15-positions, and abbreviated as $(C_nO)_m$-BTPM ($n=12$, 16; $m=4$, 8). Compounds **7** and **8** are 5,15-bis(3,4-didodecyloxyphenyl)porphyrin [abbreviated as $(C_{12}O)_4$-$BPPH_2$] and 5,15-bis(4-dodecyloxybiphenyl)porphyrin [abbreviated as $(C_{12}O)_2$-$BBPH_2$], respectively. Although compounds **1**–**3** are similar to type 2, the number of the long chains attached to them are two or four times as many as those of type 2. These compounds are, therefore, classified as type 4. Compounds **4**–**6** have the structure in which the number of *o*-terphenyl moieties is halved compared with type 4, so that they are referred to as type 5. Compound **7** is classified as type 6, because the number of alkoxy long chains is twice those of conventional type 3. Compound **8** belongs to type 3.

We wish to report here that such a successive change of the molecular structures causes their mesophases to change from discotic columnar to discotic lamellar, and further to calamitic.

2. Results and discussion

2-1. Synthesis

The porphyrin derivatives **1**–**8** in this work have been synthesized by using synthetic routes as shown in Scheme 1–4.

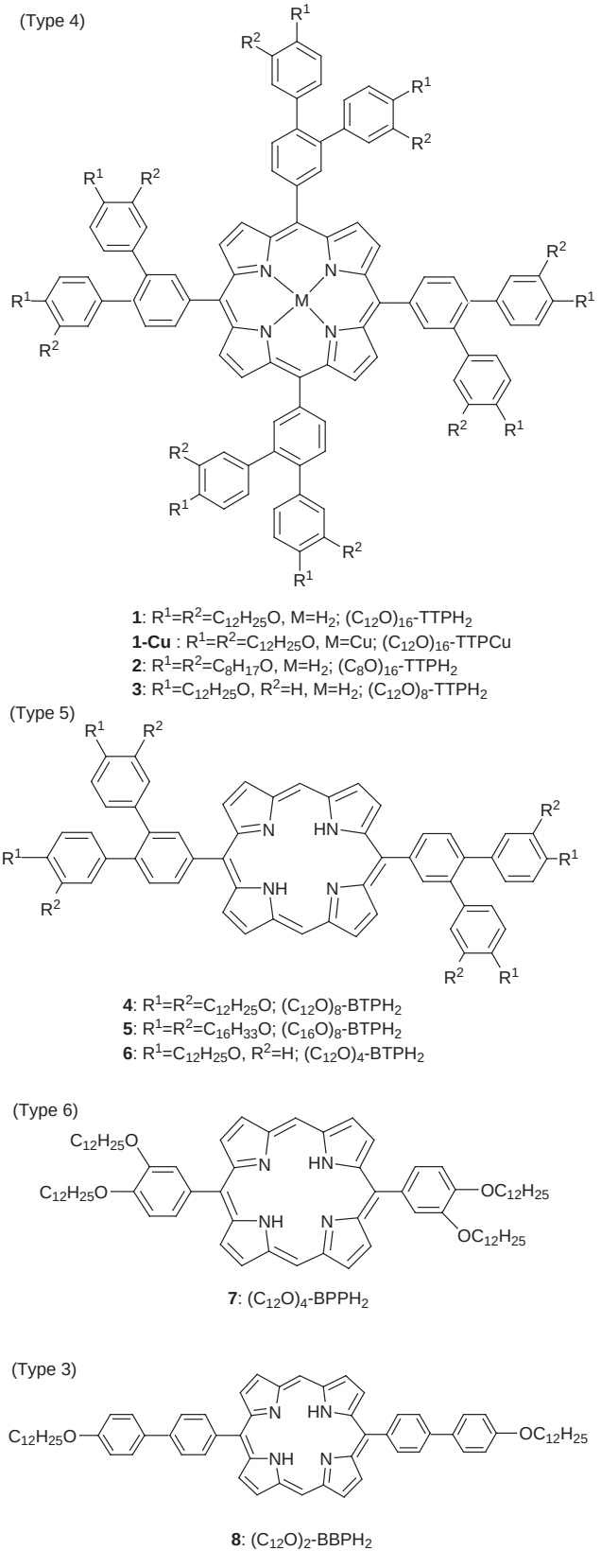

Fig. 2 Formulae of the porphyrin derivatives in this work.

In Scheme 1, the syntheses of alkoxybenzils (**13**) from the starting materials (**9**) were carried out by the method of Wenz.[19] In Scheme 2, 3,4-didodecyloxybenzaldehyde (**19**) was prepared by the method of Strzelecka *et al.*[20] 4-Bromo-4′-dodecyloxybiphenyl (**21**) was synthesized according to the procedure described by Gray *et al.*[21] The syntheses of tetrakis-substituted porphyrin derivatives **1**–**3** (Scheme 3) followed the conventional method described by Adler *et al.*,[22] and these

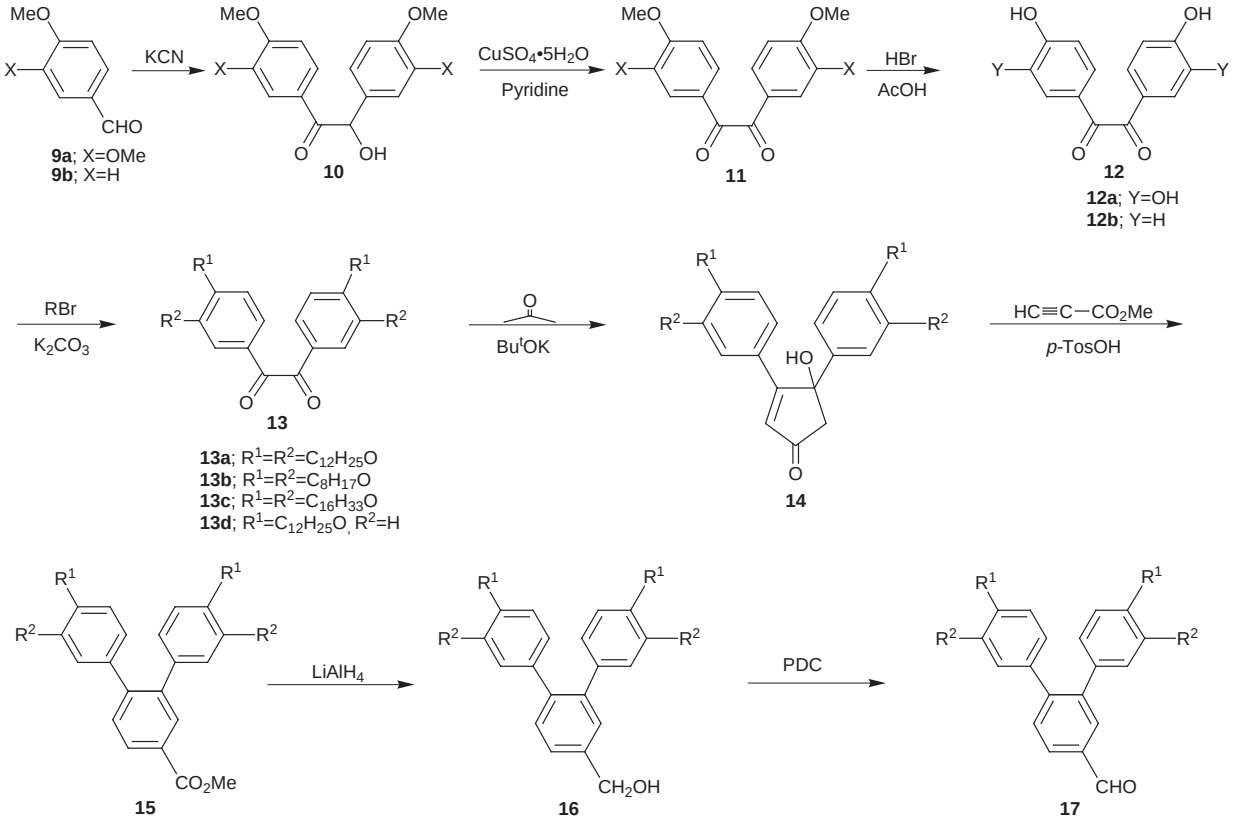

Scheme 1 Synthetic route to aldehyde **17**.

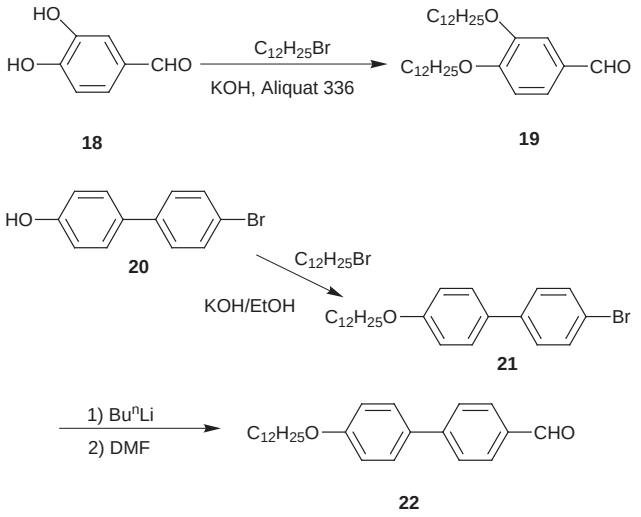

Scheme 2 Synthetic routes to aldehydes **19** and **22**.

resulting by-products, namely, chlorine derivatives were oxidized as described in the literature.[23] The copper complex (**1-Cu**) of metal free derivative **1** was obtained by the conventional synthetic procedure.[24] Bis-substituted porphyrin derivatives **4**–**8** (Scheme 4) were synthesized by using the method of Manka *et al.*[25] Further details of these synthetic procedures will be described in the Experimental section.

Elemental analysis data of the porphyrin derivatives **1**–**8** are summarized in Table 1. Electronic absorption spectral data for all of the porphyrin derivatives in this work are presented in Table 2. Each of the electronic absorption spectra showed Soret- and Q-bands which are characteristic bands of porphyrin compounds.

2-2. Liquid crystalline properties

2-2-1. $(C_nO)_m$-TTPM (1, 1-Cu, 2 and 3, type 4). Phase transition temperatures and enthalpy changes of $(C_{12}O)_{16}$-$TTPH_2$ (**1**), $(C_{12}O)_{16}$-TTPCu (**1-Cu**), $(C_8O)_{16}$-$TTPH_2$ (**2**) and $(C_{12}O)_8$-$TTPH_2$ (**3**) are summarized in Table 3. $(C_{12}O)_{16}$-$TTPH_2$ (**1**) and $(C_{12}O)_{16}$-TTPCu (**1-Cu**) exhibit mesomorphism in the low-temperature region.

The DSC thermograms of $(C_{12}O)_{16}$-$TTPH_2$ (**1**) were very complicated. When the pristine sample of this compound was at first cooled to *ca.* −100 °C and then heated at 10 °C min^{-1}, we observed a very broad endothermic peak corresponding to the transition from the X_1 phase to the M_1 phase at *ca.* −80 °C and a comparatively large endothermic peak corresponding to the change from the M_1 phase to the isotropic liquid (IL) at 39 °C. In addition, a small endothermic peak which overlapped with the peak at 39 °C was observed at 59 °C. This peak corresponds to the clearing point of the M_2 phase. When this IL was once more cooled to *ca.* −100 °C and heated, a new broad endothermic peak appeared at *ca.* −35 °C. This peak corresponds to the transition from the X_2 phase to the M_2 phase. Besides, a comparatively small peak corresponding to the X_1–M_1 transition at *ca.* −80 °C was also observed. This result indicates that when the IL of this compound is cooled, it changes into not only the X_2 phase but also the X_1 phase to some degree. On further heating, a small endothermic peak near 39 °C appeared, followed by a broad exothermic peak due to relaxation from the IL to the M_2 phase, and a small endothermic peak due to clearing from the M_2 phase to the IL was finally observed at 59 °C. The thermogram areas of the M–IL transition varied with the non-virgin samples and their enthalpy changes were below one-tenth of that of the pristine sample. This result indicates that when a sample cleared to the IL is cooled, most of the sample remains in a supercooled liquid state because of the low cohesivity of these molecules. Relaxation of this supercooled

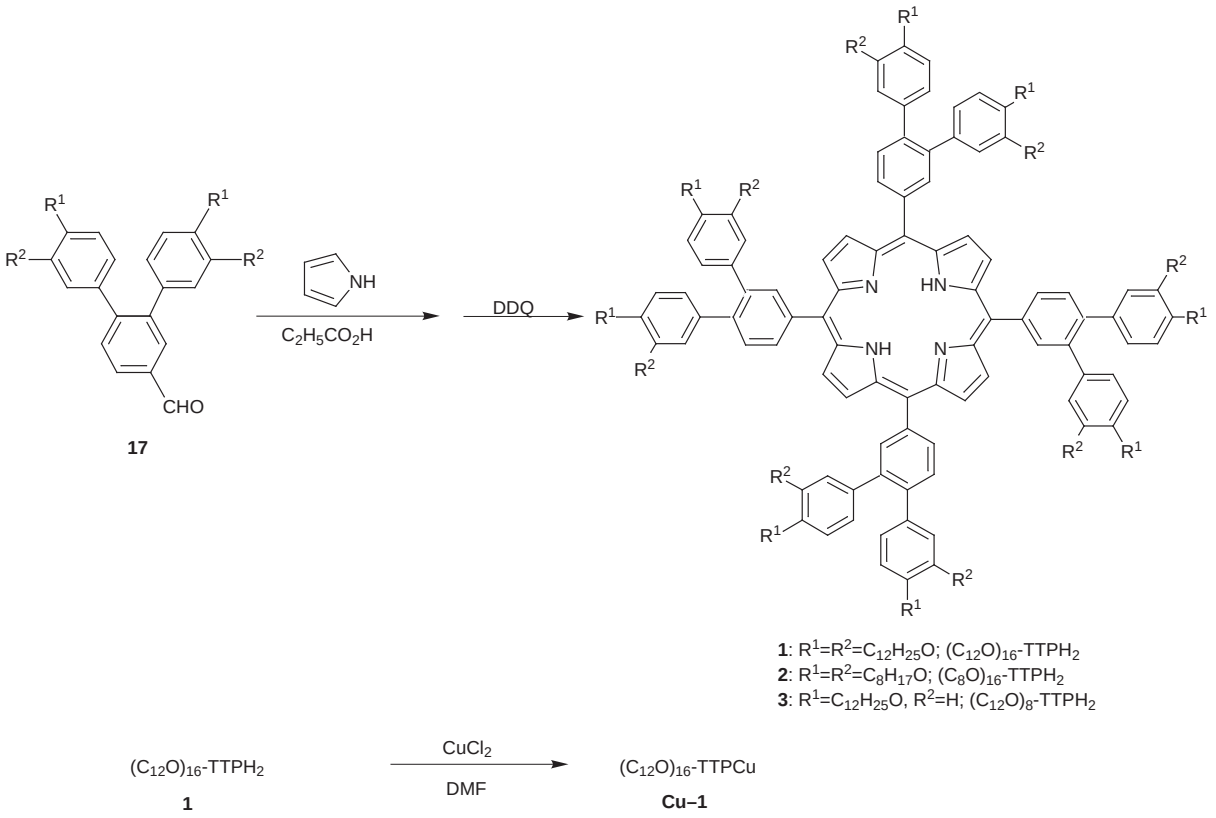

Scheme 3 Syntheses of the porphyrin derivatives **1**–**3** and the copper(II) complex of **1** (**1-Cu**).

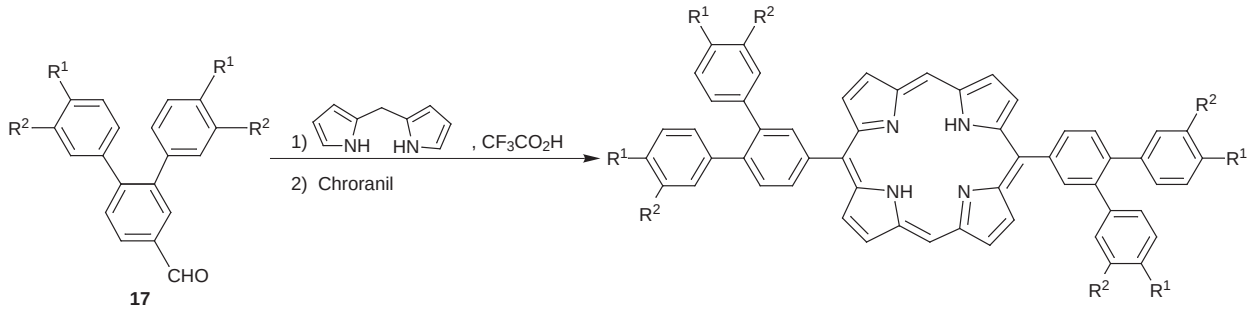

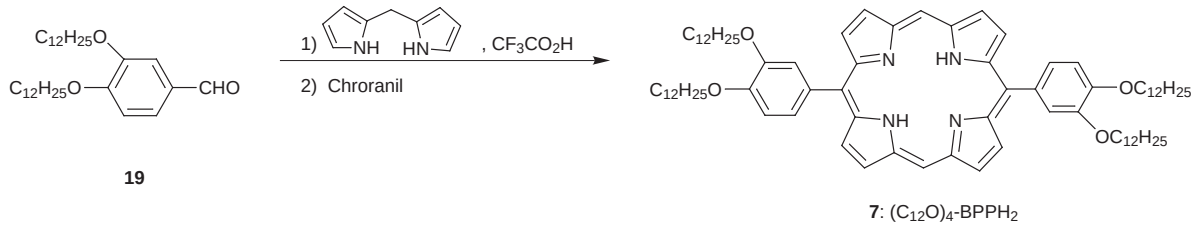

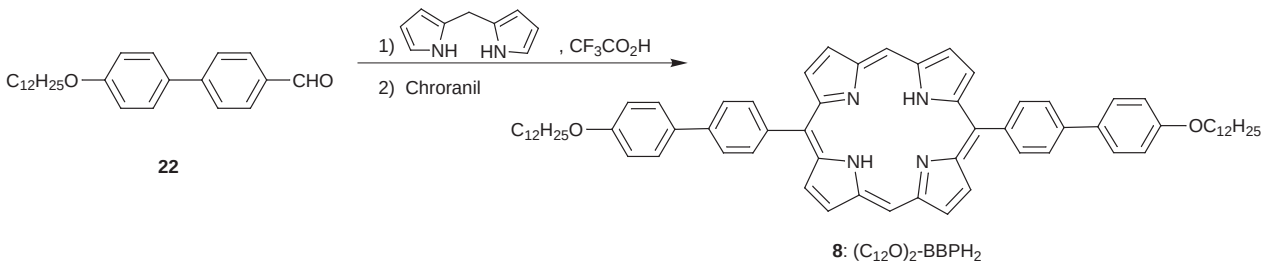

Scheme 4 Syntheses of the porphyrin derivatives **4**–**8**.

Table 1 Elemental analysis data of the porphyrin derivatives in this work

Compound	Molecular formula (molecular weight)	Found% (Calc.%)		
		C	H	N
$(C_{12}O)_{16}$-TTPH$_2$ (**1**)	$C_{284}H_{446}N_4O_{16}$ (4172.72)	81.81(81.75)	10.89(10.77)	1.18(1.34)
$(C_{12}O)_{16}$-TTPCu (**1-Cu**)	$C_{284}H_{444}N_4O_{16}Cu$ (4234.21)	80.26(80.56)	10.40(10.57)	1.16(1.32)
$(C_8O)_{16}$-TTPH$_2$ (**2**)	$C_{220}H_{318}N_4O_{16}$ (3274.99)	80.72(80.69)	9.80(9.79)	1.55(1.71)
$(C_{12}O)_8$-TTPH$_2$ (**3**)	$C_{188}H_{254}N_4O_8$ (2698.13)	83.78(83.69)	9.46(9.49)	1.99(2.08)
$(C_{12}O)_8$-BTPH$_2$ (**4**)	$C_{152}H_{230}N_4O_8$ (2241.54)	81.72(81.45)	10.36(10.34)	2.38(2.50)
$(C_{16}O)_8$-BTPH$_2$ (**5**)	$C_{184}H_{294}N_4O_8$ (2690.38)	81.94(82.15)	10.81(11.02)	1.94(2.08)
$(C_{12}O)_4$-BTPH$_2$ (**6**)	$C_{104}H_{134}N_4O_4$ (1504.23)	82.70(83.04)	8.82(8.98)	3.55(3.73)
$(C_{12}O)_4$-BPPH$_2$ (**7**)	$C_{80}H_{118}N_4O_4$ (1199.85)	80.17(80.08)	9.94(9.91)	4.26(4.67)
$(C_{12}O)_2$-BBPH$_2$ (**8**)	$C_{68}H_{78}N_4O_2$ (983.39)	83.19(83.05)	7.99(8.00)	5.74(5.70)

liquid into the M_1 phase is extremely slow; the non-pristine sample kept at room temperature (r.t.) for more than one year exhibited the same thermal behavior as the pristine sample. Considering from the results described above, the pristine state of this compound is the M_1 phase at room temperature and when it is cooled below *ca.* −80 °C it changes into the X_1 phase. When it is heated, double clearing behavior of $M_1 \rightarrow$IL—(relaxation)$\rightarrow M_2 \rightarrow$IL occurs. The X_2 phase in the non-pristine sample, which does not exist in the pristine sample, is obtained by cooling. However, the X_1 and X_2 phases are mingled to some extent in the non-pristine sample which shows, as a result, more complicated phase transition behavior.

Identification of each of the phases in the $(C_{12}O)_{16}$-TTPH$_2$ (**1**) derivative was carried out by X-ray diffraction measurements and observation of the optical textures. However, the X_1 and X_2 phases could not be identified because these two phases exist in a very low temperature region beyond the range of our instrumental techniques. The M_1 phase could be identified by using the pristine sample at r.t., and the M_2 phase could be also identified by using a sample prepared by annealing the supercooled liquid for 10 days between 39 °C (clearing point of the M_1 phase) and 59 °C (clearing point of the M_2 phase). As summarized in Table 4, the X-ray diffraction pattern of the M_1 phase of $(C_{12}O)_{16}$-TTPH$_2$ (**1**) at r.t. gave two narrow peaks in the low angle region, a fairly sharp peak in the medium angle region, and a broad halo around $2\theta = 20°$ at wide angles. The spacing ratio of the first two, low-angle peaks was $1:(1/\sqrt{3})$, which is a characteristic of two-dimensional hexagonal packing. The halo around $2\theta = 20°$ corresponds to the melting of the alkoxy chains. The fairly sharp peak in the medium angle region may correspond to a stacking distance in the columnar structure. The spacing, 9.55 Å, is twice the ordinary stacking distance, 3.5–4.7 Å, for columnar mesophases, so that it may be an interdimer distance. In this mesophase, dimerization may occur.

We have calculated the number of molecules, Z, in the two-dimensional hexagonal lattice with the possible interdimer distance h ($a = 41.5$ Å, $h = 9.55$ Å) by the following equation:

$$Z = \rho VL/M$$

where ρ is the density; V, the unit cell volume; L, Avogadro's number; and M, the molecular weight. Generally, it is considered that the density of a compound in the liquid crystalline state is 0.9–1.0 g cm^{-3}. Thereby, the density ρ of the present compound **1** in the mesophase at 125 °C is assumed as 1 g cm^{-3}.

$$\begin{aligned} V &= (\sqrt{3}/2)a^2h \\ &= (\sqrt{3}/2) \times 45.1^2 \times 9.55 \text{ Å}^3 \\ &= 1.42 \times 10^{-20} \text{ cm}^{-3} \\ Z &= 1 \times 1.42 \times 10^{-20} \times 6.02 \times 10^{23}/4172.72 \\ &= 2.05 \end{aligned}$$

Thus, we could confirm that two molecules exist in the unit cell. This means that the dimers stack with a periodicity of 9.55 Å in the column. Hence, this phase could be assigned as a discotic hexagonal ordered columnar (D_{ho}) mesophase. When this sample was heated to 55 °C and then annealed at this temperature overnight to make the M_2 phase, the X-ray diffraction pattern showed two reflections in the low angle region, a very broad and weak halo in middle angle region, and a broad and big halo around $2\theta = 20°$ in the wide angle region. From the spacing ratio of the first peaks in the low

Table 2 Electronic absorption spectral data of the porphyrin derivatives in chloroform

Compound	Concentration/ 10^{-6} mol l^{-1}	λ_{max}/nm(log ε)	
		Soret band	Q band
$(C_{12}O)_{16}$-TTPH$_2$ (**1**)	5.92	426.9(5.71)	520.4(4.32), 557.2(4.18), 594.0(3.82), 649.8(3.85)
$(C_{12}O)_{16}$-TTPCu (**1-Cu**)	6.10	422.4(5.71)	541.6(4.42), 579.0(3.75)
$(C_8O)_{16}$-TTPH$_2$ (**2**)	6.23	426.9(5.68)	520.4(4.28), 557.1(4.15), 594.2(3.77), 650.4(3.80)
$(C_{12}O)_8$-TTPH$_2$ (**3**)	6.45	426.6(5.69), 462.3(4.46)	519.7(4.27), 556.9(4.17), 594.2(3.83), 650.7(3.92), 678.4(3.92)
$(C_{12}O)_8$-BTPH$_2$ (**4**)	5.36	412.7(5.46)	505.6(4.17), 542.4(4.07), 578.0(3.83), 632.5(3.49)
$(C_{16}O)_8$-BTPH$_2$ (**5**)	6.18	411.8(5.51)	504.9(4.27), 540.2(4.04), 576.4(3.86), 631.7(3.62)
$(C_{12}O)_4$-BTPH$_2$ (**6**)	6.56	411.7(5.58)	504.6(4.25), 540.5(3.98), 576.7(3.78), 631.7(3.48)
$(C_{12}O)_4$-BPPH$_2$ (**7**)	5.58	412.5(5.58), 443.2(sh, 4.27)	504.9(4.30), 542.2(4.19), 580.4(4.06), 636.2(3.78)
$(C_{12}O)_2$-BBPH$_2$ (**8**)	6.48	411.4(5.59)	504.7(4.23), 540.0(3.97), 577.5(3.73), 631.9(3.36)

Table 3 Phase transition temperatures and enthalpy changes of the porphyrin derivatives, **1**–**8**

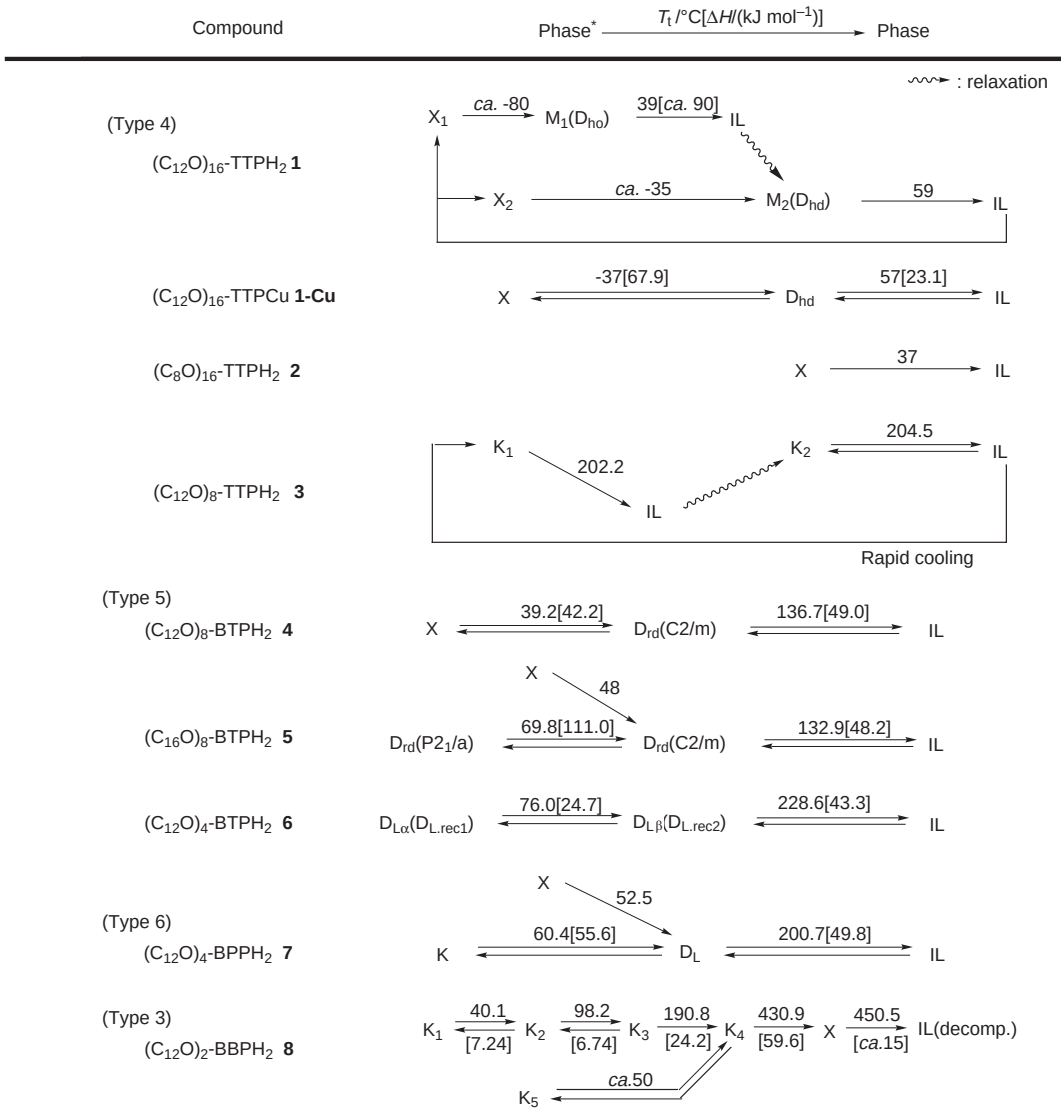

Phase nomenclature: K = crystal, D_{hd} = discotic hexagonal disordered columnar mesophase, D_{rd} = discotic rectangular disordered columnar mesophase, D_L = discotic lamellar mesophase, X = unidentified phase, and IL = isotropic liquid.

angle region and the halo around $2\theta = 20°$, this higher-temperature phase could be also assigned as a D_h mesophase, the same as the lower-temperature phase. In contrast to the lower-temperature D_h mesophase, the higher one showed a very broad and weak halo in the middle angle region which corresponds to the dimer-stacking distance. In this mesophase, the stacking distance fluctuates greatly, so that we assigned this phase as a D_{hd} mesophase. However, we could still see the halo corresponding to the stacking distance. It is very difficult to distinguish between D_{ho} and D_{hd} mesophases for such a case. Therefore, we tentatively assigned these lower- and higher-temperature mesophases as D_{ho} and D_{hd}, respectively (Table 4). When the IL was held at 58 °C, a focal-conic texture appeared for the D_h phase [Fig. 3(a)]. This texture is often observed in D_h mesophases.

As summarized in Table 3, $(C_{12}O)_{16}$-TTPCu (**1-Cu**) showed rather more simple phase transition behavior than the metal-free compound **1**, and its clearing point is nearly the same as that of the D_{hd} phase of **1**. From the results of X-ray diffraction measurements at r.t. (Table 4), this phase could be identified as a D_{hd} mesophase. When the IL of $(C_{12}O)_{16}$-TTPCu (**1-Cu**) was held for some time, a focal-conic texture appeared in the same way as its metal-free compound **1**.

For the $(C_8O)_{16}$-TTPH$_2$ (**2**) derivative, only a very small endothermic peak was observed at 37 °C in the DSC thermogram: 5.55 kJ mol^{-1} for the first heating run and 2.15 kJ mol^{-1} for the second heating run. Under a polarizing microscope, it showed an almost isotropic texture with very weak birefringence. When the cover glass was pressed, it was too rigid to slip. For the X-ray diffraction study, only two broad reflections were observed in the low and wide angle regions. Therefore, this state is thought to be a glassy liquid phase[26] or a supercooled liquid with a slightly crystallized portion. The crystalline part may melt at 37 °C. The enthalpy change depended on the degree of crystallization, as mentioned above. Since a glassy transition point was not detected by DSC measurements, this state my be a supercooled isotropic liquid state with a partially crystallized portion.

As summarized in Table 3, $(C_{12}O)_8$-TTPH$_2$ (**3**) has very high melting points in comparison with **1** and **2** having sixteen long chains. Though the derivative **3** exhibits no mesomorphism, it shows double-melting behavior in a narrow temperature region.

Type 2 *meso*-substituted porphyrin derivatives with bulky substituents (in Fig. 1) which have been reported to date show not columnar mesophases but lamellar mesophases.[13,27,28] Although type 4 $(C_{12}O)_{16}$-TTPH$_2$ (**1**) and $(C_{12}O)_{16}$-TTPCu (**1-Cu**) derivatives have larger steric hindrance groups than

Table 4 X-Ray diffraction data of the porphyrin derivatives **1**–**8**

Compound	Peak No.	Spacing (Å) $d_{observed}$	Spacing (Å) $d_{calculated}$	Miller indices (*hkl*)	Phase Lattice constant
$(C_{12}O)_{16}$-TTPH$_2$ (**1**) at r.t.[a]	1	36.0	36.0	(100)	D_{ho}
	2	21.4	20.8	(110)	
	3	9.55	sharp	(001)	$a=41.5$ Å
	4	*ca.* 4.3	—	—[b]	$h=9.55$ Å, $Z=2$
at 55 °C	1	34.4	34.4	(100)	D_{hd}
	2	19.9	19.9	(110)	
	3	*ca.* 9.1	broad	(001)	$a=39.7$ Å
	4	*ca.* 4.4	—	—[b]	$h=ca.$ 9.1 Å
$(C_{12}O)_{16}$-TTPCu(**1-Cu**) at r.t.	1	36.3	36.3	(100)	D_{hd}
	2	21.2	20.9	(110)	
	3	*ca.* 9.3	broad	(001)	$a=41.9$ Å
	4	*ca.* 4.4	—	—[b]	$h=ca.$ 9.1 Å
$(C_{12}O)_8$-BTPH$_2$ (**4**) at 125 °C	1	33.2	33.2	(110)	D_{rd} ($C2/m$)
	2	29.8	29.8	(200)	
	3	16.6	16.6	(220)	$a=59.7$ Å
	4	*ca.* 4.4	—	—[b]	$b=40.0$ Å
$(C_{16}O)_8$-BTPH$_2$ (**5**) at 60 °C	1	37.0	37.0	(200)	D_{rf} ($P2_1/a$)
	2	34.8	34.8	(110)	
	3	18.8	19.1	(120)	$a=74.1$ Å
	4	13.4	13.5	(420)	$b=39.4$ Å
	5	10.7	10.7	(430)	
	6	4.41	—	—[c]	
	7	4.14	—	—[c]	
at 120 °C	1	41.7	41.7	(110)	D_{rd}($C2/m$)
	2	36.3	36.3	(200)	
	3	22.0	21.9	(310)	$a=72.6$ Å
	4	10.5	10.4	(440)	$b=51.0$ Å
	5	*ca.* 4.6	—	—[b]	
$(C_{12}O)_4$-BTPH$_2$ (**6**) at r.t.	1	34.9	34.2	(001)	$D_{L\alpha}(D_{L.rec1})$
	2	16.7	17.1	(002)	
	3	11.0	11.0	(010)	$a=16.1$ Å
	4	9.10	9.10	(110)	$b=11.0$ Å
	5	5.40	5.37	(300)	$c=34.2$ Å
	6	4.79	4.83	(310)	$Z=2$
	7	4.53	4.55	(220)	
	8	*ca.* 4.1	—	—[b]	
Alternative assignment at r.t.	1	34.9	34.2	(001)	$D_{L\alpha}(D_{L.rec1})$
	2	16.7	17.1	(002)	
	3	11.0	11.0	(100)	$a=11.0$ Å
	4	9.10	9.10	(010)	$b=9.1$ Å
	5	5.40	5.52	(200)	$c=34.2$ Å
	6	4.79	4.72	(210)	
	7	4.53	4.55	(020)	$Z=1$
	8	*ca.* 4.1	—	—[b]	
at 220 °C	1	39.7	39.3	(001)	$D_{L\beta}(D_{L.rec2})$
	2	19.7	19.7	(002)	
	3	12.9	13.1	(003)	$a=18.6$ Å
	4	10.9	10.9	(010)	$b=10.9$ Å
	5	9.40	9.40	(110)	$c=39.3$ Å
	6	6.38	6.19	(300)	$Z=2$
	7	*ca.* 5.0	—	—[b]	
Alternative assignment at 220 °C	1	39.7	39.3	(001)	$D_{L\beta}(D_{L.rec2})$
	2	19.7	19.7	(002)	
	3	12.9	12.9	(010)	$a=19.2$ Å
	4	10.9	10.7	(110)	$b=12.8$ Å
	5	9.40	9.60	(200)	$c=39.3$ Å
	6	6.38	6.40	(020)	
	7	*ca.* 5.0	—	—[b]	$Z=4$

[a]Measured in virgin state. [b]Halo of melting of alkyl chain. [c]See the main text.

type 2 derivatives, they show D_h mesophases as described above. This may be attributed to the sixteen melting long alkyl chains which completely fill the space around the porphyrin core to allow the molecules to form a columnar assembly. In conclusion of this section, the $(C_{12}O)_{16}$-TTPH$_2$ (**1**) and $(C_{12}O)_{16}$-TTPCu (**1-Cu**) derivatives are the first examples of tetraphenylporphyrin derivatives exhibiting D_h mesophases.

Generally speaking, in type 1 porphyrin derivatives with long chains at the β-positions of the pyrrole rings, the metal-free compounds tend to show no mesomorphism whereas the metal complexes tend to exhibit columnar mesophases.[8,12] On the other hand, in type 2 *meso*-substituted derivatives, both the metal-free and metal compounds frequently have the same mesophase (in most cases D_L mesophase).[13,27,28] In this work, both the metal-free compound **1** and its copper complex **1-Cu** show the same D_{hd} mesophase. Thus, the effect of the central

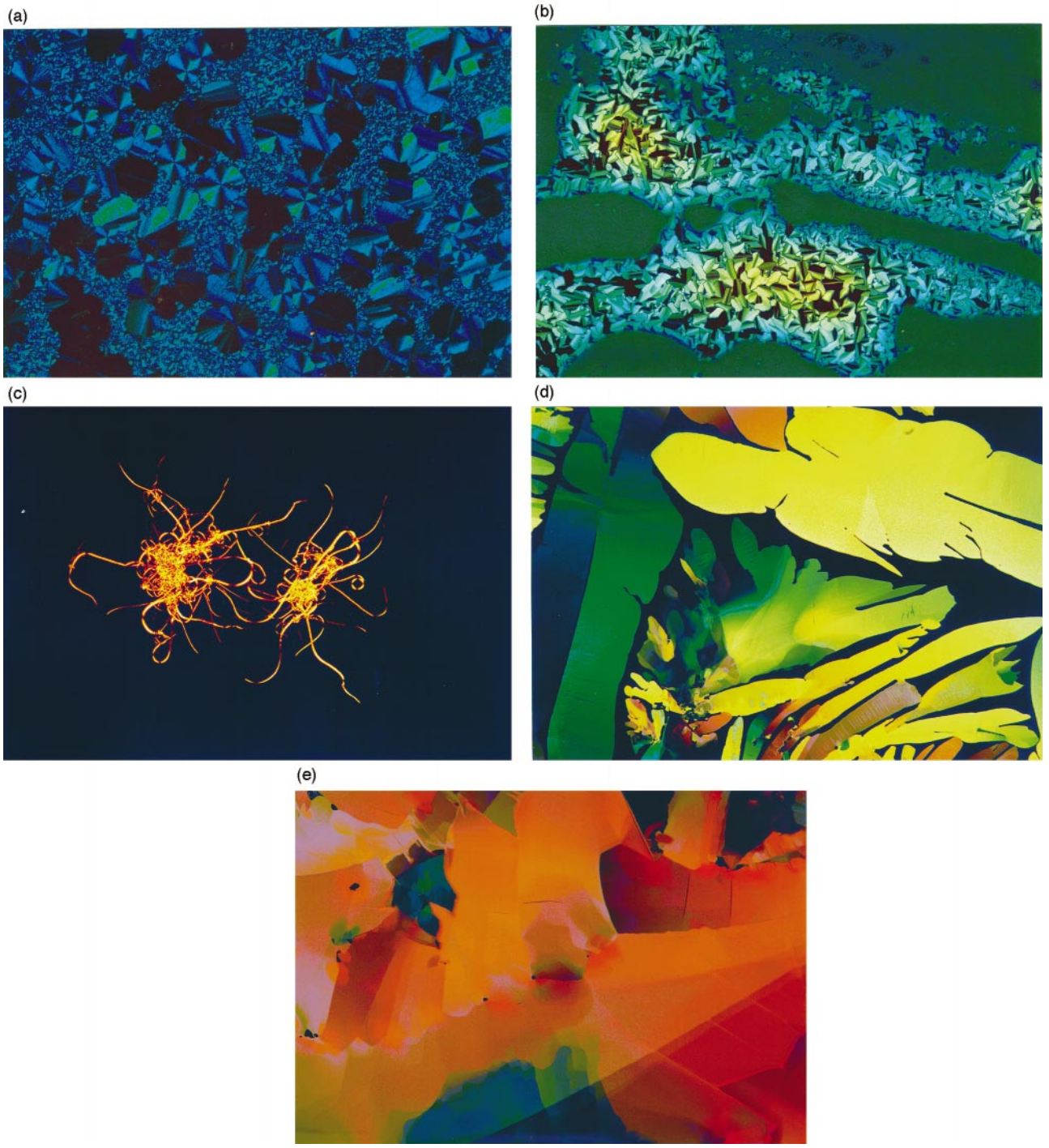

Fig. 3 Photomicrographs of (a) the D_{hd} mesophase of $(C_{12}O)_{16}$-$TTPH_2$ (**1**) at 58 °C, (b) the D_{hd} mesophase of $(C_{12}O)_{16}$-TTPCu (**1-Cu**) at 56 °C, (c) whiskers of the D_{rd} (C_2/m) mesophase of $(C_{12}O)_8$-$BTPH_2$ (**4**) at 136 °C, (d) the $D_{L\beta}$ mesophase of $(C_{12}O)_4$-$BTPH_2$ (**6**) at 226 °C, and (e) the D_L mesophase of $(C_{12}O)_4$-$BPPH_2$ (**7**) at 198 °C.

metal on the mesomorphism in type 2 and 4 compounds may be negligible Hence, we synthesized only metal-free compounds and studied their mesomorphism in our subsequent work.

2-2-2. $(C_nO)_m$-$BTPH_2$ (4, 5, and 6; type 5). Table 3 also summarizes the phase transition temperatures and the enthalpy changes of $(C_{12}O)_8$-$BTPH_2$ (**4**), $(C_{16}O)_8$-$BTPH_2$ (**5**) and $(C_{12}O)_4$-$BTPH_2$ (**6**). All the type 5 compounds **4**–**6** synthesized here exhibit mesomorphism.

$(C_{12}O)_8$-$BTPH_2$ (**4**) shows an unidentified phase (denoted as X phase) at r.t. On heating, this X phase transforms to a D_{rd} ($C2/m$) mesophase at 39.2 °C, and it clears to the IL at 136.7 °C. The values of the enthalpy changes for these two phase transitions are roughly the same. The X-ray diffraction pattern for this compound at 125 °C (Table 4) gave three narrow peaks in the low angle region and a diffuse band around $2\theta = 20°$ which correspond to the melting of alkyl chains. This phase could be then assigned to a discotic rectangular disordered columnar (D_{rd}) mesophase. Furthermore, it was established from the extinction rules in two-dimensional rectangular lattices that this D_{rd} mesophase has $C2/m$ symmetry (Table 4).

$(C_{16}O)_8$-$BTPH_2$ (**5**) in the pristine state at room temperature is a mixture of an unidentified phase (X phase) and a D_{rd} ($P2_1/a$) mesophase. The X and D_{rd} ($P2_1/a$) phases both change into a D_{rd} ($C2/m$) phase at 48 and 69.8 °C, respectively. The X phase does not appear without the first heating run. The X-ray diffraction pattern for this compound at 120 °C showed

four narrow peaks in the low angle region and a broad fifth peak 5 around $2\theta = 20^\circ$ (Table 4). This phase could be assigned to a D_{rd} ($C2/m$) mesophase. It is the same phase as that in $(C_{12}O)_8$-$BTPH_2$ (**4**). When the sample was heated to clear, and then cooled to r.t., it gave a pure mesophase. The X-ray diffraction pattern of the mesophase at 60 °C gave seven narrow peaks (Table 4). From five peaks in the low angle region, this phase could be assigned to a D_{rd} ($P2_1/a$) mesophase. The remaining two peaks at wide angles could not be assigned to reflections from the two-dimensional rectangular $P2_1/a$ lattice. They probably indicate that the long aliphatic chains partially crystallize within the intercolumnar space, similarly to the D_h phase of bis(octaoctadecylphthalocyaninato)lutetium complex.[29]

When the IL of $(C_{12}O)_8$-$BTPH_2$ (**4**) was held for a few hours just below its clearing point, 'whisker growth' was observed [Fig. 3(c)]. Although the materials which were reported to form whiskers are mainly inorganic compounds, polymers such as poly(4-hydroxybenzoate)[30] and organic compounds such as L-alanine[31] were also reported to form whiskers. Generally, crystal whiskers are needle-like, whereas the whisker in the case of $(C_{12}O)_8$-$BTPH_2$ (**4**) is bent. Bending of whiskers has been described to be caused by characteristic defects in structures composed of stacks of disc-like molecules,[32] so that it can evidence the columnar mesomorphism of $(C_{12}O)_8$-$BTPH_2$ (**4**). Another example of such bent whiskers has been reported in 2,4,6-tris(didecylamino)-*s*-triazine.[32] The same whiskers could be also seen for the homologous $(C_{16}O)_8$-$BTPH_2$ (**5**) derivative under similar conditions to the $(C_{12}O)_8$-$BTPH_2$ (**4**) derivative, although the whiskers were not so large in **5**.

Both $(C_{12}O)_8$-$BTPH_2$ (**4**) and $(C_{12}O)_4$-$BTPH_2$ (**6**) are classified as type 5, although **4** and **6** have eight and four long chains (dodecyloxy groups), respectively. As summarized in Table 3, $(C_{12}O)_4$-$BTPH_2$ (**6**) shows a transformation from the $D_{L\alpha}$ to the $D_{L\beta}$ phase at 76.0 °C (subscripts α and β are used not to express phase features but only to distinguish the different phases), and $D_{L\beta}$ clears to the IL at 228.6 °C. The clearing point of this compound is *ca.* 90 °C higher than those of $(C_{12}O)_8$-$BTPH_2$ (**4**) and $(C_{16}O)_8$-$BTPH_2$ (**5**), and the stability of the mesophase rises. As summarized in Table 4, the X-ray diffraction pattern of $(C_{12}O)_4$-$BTPH_2$ (**6**) at 220 °C gave seven peaks. Since peak 7 was broad, it corresponds to melting of the alkyl chains. The ratio of the spacings of peaks 1–3 in the low angles is 1 : 1/2 : 1/3, which represents the existence of lamellar structure. The remaining peaks 4–6 could be assigned to the reflections from a two-dimensional rectangular lattice. Hence this mesophase was proven to be a lamellar mesophase having two-dimensional rectangular order within the layer ($D_{L\beta} = D_{L.rec.2}$). Besides, from the X-ray diffraction data at r.t., the $D_{L\alpha}$ phase is also a lamellar mesophase with two-dimensional rectangular order within the layer (Table 4, $D_{L\alpha} = D_{L.rec.1}$). Interestingly, alternative two-dimensional lattice constants, 11.0 Å × 9.10 Å and 19.2 Å × 12.8 Å, also fit well for $D_{L\alpha}$ at r.t. and for $D_{L\beta}$ at 220 °C, respectively, as listed in Table 4. Generally, a limited number of sharp peaks in mesophases make it difficult to reach an unambiguous two-dimensional lattice assignment. Further investigation is required for the detailed structural differences between these $D_{L\alpha}$ and $D_{L\beta}$ phases. We recently found two novel discotic lamellar $D_{L.rec}$ mesophases,[33] whose structures in the layers may be closely related to those of the present $D_{L\alpha}$ and $D_{L\beta}$ mesophases.

As shown in Fig. 3(d), the terrace texture with piles of plates could be observed under a polarizing microscope when the IL of $(C_{12}O)_4$-$BTPH_2$ (**6**) was slowly cooled to 226 °C. This indicates the existence of lamellar structure in the $D_{L\beta}$ mesophase. The plates in the texture were striated in the temperature region of the $D_{L\alpha}$ mesophase below 76.0 °C, but no dramatic change was observed. This also suggests that both $D_{L\alpha}$ and $D_{L\beta}$ phases have lamellar structure.

In conclusion of this section, type 5 $(C_{12}O)_8$-$BTPH_2$ (**4**) and $(C_{16}O)_8$-$BTPH_2$ (**5**) derivatives having eight long alkoxy chains show D_{rd} mesophases. On the other hand, the type 5 $(C_{12}O)_4$-$BTPH_2$ (**6**) derivative having four long alkoxy chains exhibits two $D_{L.rec.}$ mesophases. It is very interesting that the mesophases in type 5 change from the D_{rd} phase with columnar structure to the D_L phase with lamellar structure when the number of attached long alkyl chains is reduced by half. Furthermore, it was found that the D_L mesophases in the $(C_{12}O)_4$-$BTPH_2$ (**6**) derivatives have two-dimensional rectangular order within the layer.

2-2-3. $(C_{12}O)_4$-$BPPH_2$ (7; type 6). The phase transition behavior of $(C_{12}O)_4$-$BPPH_2$ (**7**) is summarized in Table 3. The pristine sample showed two endothermic peaks at 52.5 °C and 60.4 °C which were mutually overlapped in the DSC thermograms. The endothermic peak at 52.5 °C did not appear for the non-pristine sample. Thus, the pristine state of this compound at r.t. is a mixture of an unidentified X phase and a crystalline K phase. The X phase could not be characterized because the pure phase could not be obtained. The non-pristine sample showed two reproducible endothermic peaks at 60.4 °C and 200.7 °C. As can be seen in Table 3, the enthalpy change at the lower phase transition is somewhat larger than that of the higher phase transition.

The X-ray diffraction pattern of this compound at 170 °C gave large peaks in the low angle region which were characteristic of lamellar phases and the layer spacing could be calculated to be $c = 31.7$ Å. Several comparatively small peaks on a diffuse halo at wide angles could not be assigned, because these peaks became bigger and sharper during the several hours' X-ray measurements and additional peaks appeared. This phenomenon is due to relaxation from D_L to another unidentified crystalline phase.

When the IL of $(C_{12}O)_4$-$BPPH_2$ (**7**) was held at 198 °C for a few minutes, a texture with a terraced structure appeared as shown in Fig. 3(e). This indicates the existence of lamellar structure in the D_L mesophase.

As mentioned above, the X-ray diffraction pattern for $(C_{12}O)_4$-$BPPH_2$ (**7**) showed a halo corresponding to the melting of the alkyl chains around $2\theta = 20^\circ$. Accordingly, the alkyl chains seem to fluctuate in this phase. The fluctuation of the alkyl groups of **7** was then studied by means of temperature-dependent IR spectroscopy. The vibrational spectral changes of the phase transitions of *n*-paraffin[34,35] bilayer systems[36] and discotic liquid crystals[37] have been reported. The temperature dependence of the methylene rocking band of phase II ('rotator' or 'hexagonal'[38] phase) of *n*-paraffins has been studied in detail, because this band which usually appears near 720 cm^{-1} is very sensitive to structural changes caused by phase transitions.

The crystalline state of **7** showed two bands near 745 and 723 cm^{-1} at 30 °C. The band near 720 cm^{-1} is usually assigned to the methylene rocking mode in all-*trans* alkyl chains. It splits into two bands in the solid state because of factor group splitting. The interval (*ca.* 22 cm^{-1}) between these two bands is fairly wide in comparison with general splitting width (*ca.* 10 cm^{-1}) of the well-discussed factor group splitting.[35,36,38] Therefore, it seems that the two bands of the present case are not usual. Snyder[39] reported that the methylene rocking band of molten polyethylene had been graphically resolved into two components at 719 cm^{-1} and 745 cm^{-1}, and that the higher-frequency component at 745 cm^{-1} was near the value calculated for alternating *trans–gauche* sequences. Hence, this compound at 30 °C may have a considerable proportion of *gauche* bonds in the aliphatic chains, as is the case in the references mentioned above.

The ratios of the absorbances of the two bands for **7** are plotted against temperature in Fig. 4. When the sample was heated to 60.4 °C above the melting point of **7**, the intensity

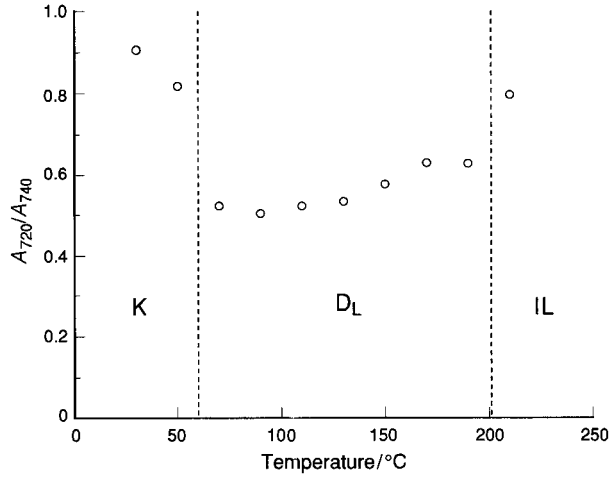

Fig. 4 Temperature dependence of the absorption ratio of two methylene rocking bands at *ca.* 720 and 740 cm^{-1} (A_{720}/A_{740}) for $(C_{12}O)_4$-$BPPH_2$ (**7**).

of the lower-frequency band at *ca.* 723 cm^{-1} suddenly decreased, and the higher-frequency band at *ca.* 745 cm^{-1} slightly shifted to lower frequency. On further heating, the bands gradually broadened, and a broad band remained at 734 cm^{-1} in the isotropic liquid at 210 °C. The ratio discontinuously altered at the melting point. As can be seen in Fig. 4, the absorption band at 723 cm^{-1} suddenly decreased at the phase transition. This may suggest that some *trans* bonds of the methylene groups change into *gauche* bonds upon heating to break all-*trans* sequences. The broadening of the bands may be due to disorder of the alkyl chains melted by heating. However, since *trans* bonds in *n*-hydrocarbons are normally more stable than *gauche* bonds, the absorption of *trans* bonds should be more intense than *gauche* ones. In the molten state, *e.g.*, liquid *n*-paraffin and molten polyethylene, all-*trans* methylene rocking bands remain fairly even when they broaden. An explanation for the difference between the conventional results and the present results has not been obtained. Nevertheless, it is at least supported that the long alkyl chains of **7** are fairly disordered in the liquid crystalline state of the D_L phase.

2-2-4. $(C_{12}O)_2$-$BBPH_2$ (8; type 3). In an attempt to obtain a calamitic mesophase in porphyrin derivatives, a rod-like $(C_{12}O)_2$-$BBPH_2$ (**8**) derivative was synthesized. The phase transition behavior of $(C_{12}O)_2$-$BBPH_2$ (**8**) is summarized in Table 3. It was revealed by means of DSC measurements that this compound shows many phase transitions, and that it finally showed an endothermic peak at 450.5 °C which may be assigned to the clearing point with decomposition. All the phases exhibited below 300 °C turned out to be crystalline phases according to polarizing microscopic observations and X-ray diffraction study. The phase between 430.9 °C and 450.5 °C, only detected by DSC measurements, could not be identified because of the high temperature which exceeds our instrumental limits. Consequently, this phase is termed an X phase. The possibility of mesomorphism of this X phase still remains because the value of ΔH at the X→IL transition is smaller than that at the K_4→X transition. This compound has a highly rigid molecule in comparison with the aforementioned compounds exhibiting mesomorphism. Thus, $(C_{12}O)_2$-$BBPH_2$ (**8**) retains its crystal structure even at high temperature.

3. Conclusion

We have synthesized nine novel porphyrin derivatives, **1**–**8** and **1-Cu**, substituted with various steric hindrance groups and long flexible chains in order to investigate their mesomorphism.

Fig. 5 summarizes the relationship between the molecular type of porphyrin derivatives, **1**–**8** and **1-Cu**, and the resulting mesophase. Type 4 disc-like $(C_{12}O)_{16}$-$TTPH_2$ (**1**) and $(C_{12}O)_{16}$-TTPCu (**1-Cu**) derivatives exhibit D_h columnar mesophases, which are the first examples of *meso*-substituted porphyrin metal-free derivatives and copper complexes. Type 5 strip-like $(C_nO)_8$-$BTPH_2$ [**4** ($n=12$), **5** ($n=16$)] derivatives having eight long chains at the 5,15-positions show the D_{rd} columnar mesophases. On the other hand, type 5 $(C_{12}O)_4$-$BTPH_2$ (**6**) derivative having four long chains exhibits $D_{L.rec1}$ and $D_{L.rec2}$ lamellar mesophases which have two-dimensional rectangular structure within the layer. The $(C_{12}O)_4$-$BPPH_2$ (**7**) derivative, of type 6, also shows a D_L lamellar mesophase. Bruce *et al.*[17] reported that the type 3 rod-like porphyrin derivatives show calamitic mesophases of S_B, S_E and $S_{E'}$ phases. As can be seen from the top derivative to the bottom one in Fig. 5, it is, therefore, apparent that such a successive change of the molecular structures causes their mesophases to change from discotic columnar to discotic lamellar, and further to calamitic. It is also apparent that the porphyrin core is very useful to obtain various kinds of mesomorphism from discotic to calamitic with alteration of the substituted positions and/or substituents.

4. Experimental

4-1. Measurements

The products synthesized here were identified by ^1H NMR (JOEL JNM-$PMX60_{SI}$) and IR (Jasco A-100). Further identification of the porphyrin derivatives was made by elemental analysis (Perkin-Elmer elemental analyzer 240B) and electronic absorption spectroscopy (Hitachi 330 spectrophotometer).

The phase transition behaviors of these compounds were observed by using a polarizing microscope (Olympus BH2), equipped with a heating plate controlled by a thermoregulator (Mettler FP80 and FP82), and differential scanning calorimetry (Shimadzu DSC-50 and Rigaku Thermoflex DSC-8230). The X-ray diffraction measurements were performed with Cu-Kα radiation (Rigaku Geigerflex) equipped with a hand-made heating plate[40] controlled by a thermoregulator. Temperature-dependent infrared spectra were measured by a Jasco FT/IR-7300 instrument equipped with a hand-made heating plate[41] controlled by a thermoregulator for a thin film of $(C_{12}O)_4$-$BPPH_2$ (**7**). This thin film was prepared by casting from a dichloromethane solution on a silicon wafer, then the solvent was removed by heating, and the film covered by another wafer.

4-2. Synthesis

3,4-Bis(3,4-didodecyloxyphenyl)-4-hydroxycyclopent-2-en-1-one(14a). This compound was synthesized by a similar method as described in previous papers.[42,43]

14a: Purified by column chromatography (silica gel, chloroform–ethyl acetate 5:1; $R_f=0.68$). Yellow liquid crystal (S_A). Clearing point (c.p.) 55 °C (lit.[43] 54 °C). Yield 74%. ^1H NMR ($CDCl_3$, TMS) δ 0.90 (m, 12H, CH_3), 1.27 (m, 80H, CH_2), 2.73 (s, 2H, CH_2CO), 3.40–4.06 (m, 9H, OH and OCH_2), 6.27 (s, 1H, =CHCO), 6.43–7.03 (m, 6H, Ph). IR(neat) ν_{max} 3400 (OH), 2930, 2860 (CH_2), 1680 (CO), 1590, 1510 (Ph), 1260 cm^{-1} (ROPh).

14b: Purified by column chromatography (silica gel, chloroform–ethyl acetate 5:1; $R_f=0.60$). Yellow liquid crystal (S_A). c.p. 42.5 °C. Yield 55%. ^1H NMR (CCl_4, TMS) δ 0.85 (m, 12H, CH_3), 1.30 (m, 48H, CH_2), 2.67 (s, 2H, CH_2CO), 3.47 (s, 1H, OH), 3.57–3.97 (m, 8H, OCH_2), 6.23 (s, 1H, =CHCO), 6.37–7.10 (m, 6H, Ph). IR (neat) ν_{max} 3350 (OH),

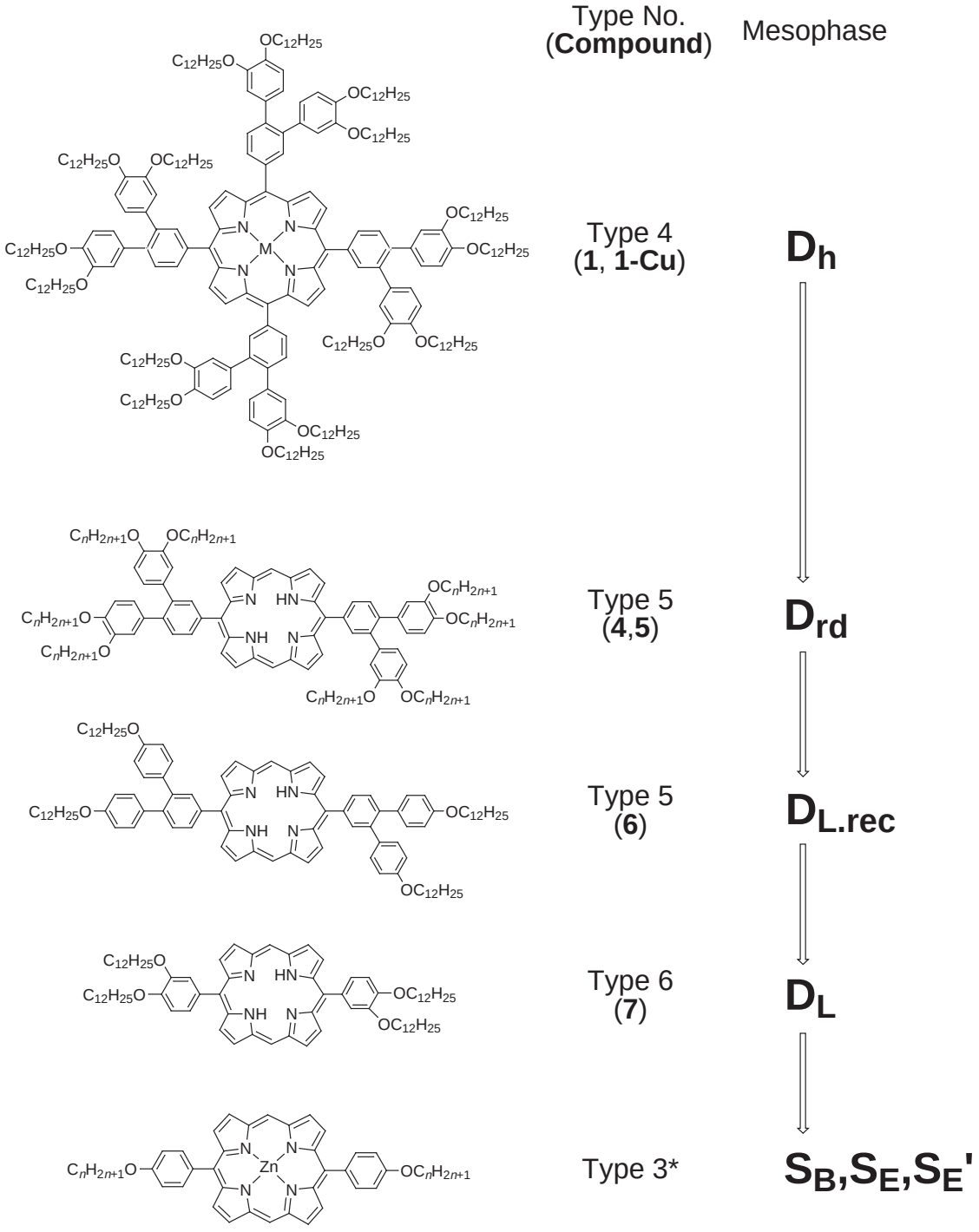

Fig. 5 The relationship between the molecular type of porphyrin derivatives and the resulting mesophase. (*see ref. 17).

2930, 2860 (CH_2), 1675 (CO), 1590, 1510 (Ph), 1260 cm^{-1} (ROPh).

14c: Purified by column chromatography (silica gel, chloroform–ethyl acetate 5:1; R_f=0.74). Yellow solid. m.p. 56–57 °C. Yield 62%. ^1H NMR ($CDCl_3$, TMS) δ 0.83 (m, 12H, CH_3), 1.20 (m, 112H, CH_2), 2.80 (s, 2H, CH_2CO), 3.57 (s, 1H, OH), 3.80 (m, 8H, OCH_2), 6.33 (s, 1H, =CHCO), 6.53–7.03 (m, 6H, Ph). IR (KBr) ν_{max} 3350 (OH), 2930, 2860 (CH_2), 1675 (CO), 1590, 1510 (Ph), 1260 cm^{-1} (ROPh).

14d: Purified by column chromatography (silica gel, chloroform–ethyl acetate 5:1; R_f=0.54). Pale yellow solid. m.p. 66–69 °C (lit.[42] 65–68 °C). Yield 49%. ^1H NMR (CCl_4, TMS) δ 0.87 (m, 6H, CH_3), 1.30 (m, 40H, CH_2), 2.70 (s, 2H, CH_2CO), 3.50 (s, 1H, OH), 3.80 (t, J=6.0 Hz, 4H, OCH_2), 6.27 (s, 1H, =CHCO), 6.47–7.57 (m, 6H, Ph). IR (neat) ν_{max} 3380 (OH), 2930, 2860 (CH_2), 1680 (CO), 1590, 1510 (Ph), 1250 cm^{-1} (OPh).

Methyl 3,4,3″,4″-tetradodecyloxy-*o*-terphenyl-4′-carboxylate (15a). A mixture of cyclopentenone **14a** (4.60 g, 4.66 mmol) and methyl propiolate (1.17 g, 13.9 mmol) in 50 ml of *o*-dichlorobenzene was heated at 70 °C. A solution of *p*-toluenesulfonic acid monohydrate (47.8 mg, 0.25 mmol) in 2 ml of 1,4-dioxane was added dropwise. The mixture was stirred for 4 h at 70 °C, and then refluxed for 8 h 40 min. The reaction mixture was extracted with chloroform. The organic layer was washed with water, dried over sodium sulfate, and the solvent was removed. The purification was carried out by column chromatography (silica gel, benzene–carbon tetrachloride 1:1; R_f=0.50), to obtain 2.24 g of **15a** as a yellowish-brown solid.

m.p. 55 °C. Yield 47%. ^{1}H NMR (CCl_4, TMS) δ 0.88 (m, 12H, CH_3), 1.27 (m, 80H, CH_2), 3.42, 3.83 (t+t, 8H, OCH_2), 3.83 (s, 3H, $COOCH_3$), 6.40–7.97 (m, 9H, Ph). IR (neat) ν_{max} 1720 cm^{-1} (CO).

15b: Purified by column chromatography (silica gel, benzene; R_f=0.60). Yellowish brown syrup. Yield 44%. ^{1}H NMR (CCl_4, TMS) δ 0.87 (m, 12H, CH_3), 1.30 (m, 48H, CH_2), 3.27–4.00 (t+t, 8H, OCH_2), 3.83 (s, 3H, $COOCH_3$), 6.33–8.00 (m, 9H, Ph). IR (neat) ν_{max} 1725 cm^{-1} (CO).

15c: Purified by column chromatography (silica gel, benzene–carbon tetrachloride 2:1; R_f=0.56). Light brown solid. m.p. 50 °C. Yield 49%. ^{1}H NMR (CCl_4, TMS) δ 0.87 (m, 12H, CH_3), 1.30 (m, 112H, CH_2), 3.40–4.00 (m, 8H, OCH_2), 3.83 (s, 3H, $COOCH_3$), 6.33–7.90 (m, 9H, Ph). IR (KBr) ν_{max} 1720 cm^{-1} (CO).

15d: Purified by column chromatography (silica gel, benzene–carbon tetrachloride 1:1; R_f=0.45). Yellowish brown syrup. Raw yield 71% (this product contained some impurities.). ^{1}H NMR (CCl_4, TMS) δ 0.90 (m, 6H, CH_3), 1.27 (m, 40H, CH_2), 3.80 (m, 7H, OCH_2, $COOCH_3$), 6.47–7.87 (m, 11H, Ph). IR (neat) ν_{max} 1725 cm^{-1} (CO).

3,4,3″,4″-Tetradodecyloxy-4′-hydroxymethyl-*o*-terphenyl (16a). Under a nitrogen atmosphere, a solution of carboxylate **15a** (2.11 g, 2.06 mmol) in 20 ml of dry diethyl ether was added dropwise to a suspension of lithium aluminium hydride ($LiAlH_4$; 0.31 g, 8.17 mmol) in 15 ml of dry diethyl ether. The mixture was gently refluxed for 1 h. After the reaction mixture was cooled by ice water, water was added slowly till no $LiAlH_4$ remained. Then, a small amount of 20% sulfuric acid was added to dissolve the precipitate, and extracted with diethyl ether. The organic layer was washed with water, dried over sodium sulfate, and concentrated. The residue was purified by column chromatography (silica gel, chloroform; R_f=0.44) to give 1.58 g of **16a** as a faintly-brown syrup. Yield 93%. ^{1}H NMR(CCl_4, TMS) δ 0.90 (m, 12H, CH_3), 1.30 (m, 80H, CH_2), 1.70 (s, 1H, OH), 3.43–4.00 (m, 8H, OCH_2), 4.60 (s, 2H, $PhCH_2O$), 6.40–7.23 (m, 9H, Ph). IR (neat) ν_{max} 3330 cm^{-1} (OH).

16b: Purified by column chromatography (silica gel, chloroform; R_f=0.21). Pale brown syrup. Yield 90%. ^{1}H NMR (CCl_4, TMS) δ 0.87 (m, 12H, CH_3), 1.30 (m, 48H, CH_2), 2.26 (s, 1H, OH), 3.30–4.00 (t+t, 8H, OCH_2), 4.58 (s, 2H, $PhCH_2O$), 6.33–7.26 (m, 9H, Ph). IR (neat) ν_{max} 3200 cm^{-1} (OH).

16c: Purified by column chromatography (silica gel, chloroform; R_f=0.38). White solid. m.p. 52 °C. Yield 67%. ^{1}H NMR (CCl_4, TMS) δ 0.88 (m, 12H, CH_3), 1.27 (m, 112H, CH_2), 1.63 (s, 1H, OH), 3.33–4.00 (m, 8H, OCH_2), 4.55 (s, 2H, $PhCH_2O$), 6.27–7.20 (m, 9H, Ph). IR (KBr) ν_{max} 3300 cm^{-1} (OH).

16d: Purified by column chromatography (silica gel, chloroform; R_f=0.40). Pale orange solid. m.p. 47.5 °C. Yield 42%. ^{1}H NMR (CCl_4, TMS) δ 0.90 (m, 6H, CH_3), 1.27 (m, 40H, CH_2), 1.93 (s, 1H, OH), 3.80 (t, J=6.0 Hz, 4H, OCH_2), 4.53 (s, 2H, $PhCH_2O$), 6.47–7.13 (m, 11H, Ph). IR (neat) ν_{max} 3330 cm^{-1} (OH).

3,4,3″,4″-Tetradodecyloxy-*o*-terphenyl-4′-carbaldehyde (17a). A mixture of hydroxymethyl **16a** (1.54 g, 1.54 mmol) and pyridinium dichromate (PDC; 0.87 g, 2.31 mmol) in 3 ml of dichloromethane was stirred for 10 h. The reaction mixture was concentrated and the residue was purified by column chromatography (silica gel, benzene; R_f=0.70) to give 1.46 g of **17a** as a yellowish white solid. m.p. 64–65 °C. Yield 95%. ^{1}H NMR (CCl_4, TMS) δ 0.88 (m, 12H, CH_3), 1.30 (m, 80H, CH_2), 3.40–4.13 (m, 8H, OCH_2), 6.40–7.85 (m, 9H, Ph), 9.92 (s, 1H, CHO). IR (neat) ν_{max} 1700 cm^{-1} (CO).

17b: Purified by column chromatography (silica gel, chloroform; R_f=0.65). Brownish yellow syrup. Yield 98%. ^{1}H NMR (CCl_4, TMS) δ 0.88 (m, 12H, CH_3), 1.27 (m, 48H, CH_2), 3.17–4.00 (m, 8H, OCH_2), 6.27–7.80 (m, 9H, Ph), 9.83 (s, 1H, CHO). IR (neat) ν_{max} 1695 cm^{-1} (CO).

17c: Purified by column chromatography (silica gel, benzene; R_f=0.55). Yellowish white solid. m.p. 58 °C. Yield 93%. ^{1}H NMR (CCl_4, TMS) δ 0.88 (m, 12H, CH_3), 1.25 (m, 112H, CH_2), 3.40–4.07 (m, 8H, OCH_2), 6.37–7.80 (m, 9H, Ph), 9.87 (s, 1H, CHO). IR (KBr) ν_{max} 1695 cm^{-1} (CO).

17d: Purified by column chromatography (silica gel, benzene; R_f=0.60). Yellow syrup. Yield 95%. ^{1}H NMR (CCl_4, TMS) δ 0.90 (m, 6H, CH_3), 1.30 (m, 40H, CH_2), 3.83 (t, J=6.0 Hz, 4H, OCH_2), 6.40–7.77 (m, 11H, Ph), 9.87 (s, 1H, CHO). IR (neat) ν_{max} 1700 cm^{-1} (CO).

5,10,15,20-Tetrakis(3,4,3″,4″-tetradodecyloxy-*o*-terphenyl)-porphyrin [1; $(C_{12}O)_{16}$-TTPH$_2$]. A mixture of aldehyde **17a** (1.48 g, 1.49 mmol) and pyrrole (0.23 g, 3.43 mmol) in propionic acid (10 ml, 0.13 mol) was refluxed for 30 min. After the reaction mixture was cooled to room temperature, sodium hydroxide (5.20 g, 0.13 mol) was added. The mixture was extracted with diethyl ether, and the organic layer was washed with water. After being dried and concentrated, the residue was purified by column chromatography (alumina, benzene; R_f=1.00) to yield 0.38 g of the crude (chlorin-contained) porphyrin derivative. The crude product was dissolved in the minimum amount of chloroform and a small amount of benzene. 2,3-Dichloro-5,6-dicyano-1,4-benzoquinone (DDQ; 0.14 g, 0.62 mmol) was added, and the mixture was refluxed for 3 h. The mixture was concentrated and the residue was purified by column chromatography (silica gel, benzene; R_f=1.00, and alumina, hexane; R_f=0.00, chloroform; R_f=1.00) to give 0.22 g of **1** as a red-purple liquid crystal. Yield 14%. ^{1}H NMR ($CDCl_3$, TMS) δ −2.63 (s. 2H, NH), 0.80 (m, 48H, CH_3), 1.26 (m, 320H, CH_2), 3.44–4.10 (m, 32H, OCH_2), 6.52–8.24 (m, 36H, Ph), 8.90 (s, 8H, porphyrin). IR (neat) ν_{max} 3320 (NH), 2930, 2860 (CH_2), 1600, 1580 (Ph), 1260 cm^{-1} (ROPh).

5,10,15,20-Tetrakis(3,4,3″,4″-tetraoctyloxy-*o*-terphenyl)-porphyrin [2; $(C_8O)_{16}$-TTPH$_2$]. The title compound was synthesized from aldehyde **17b** according to the method described above, and purified by column chromatography (alumina, benzene and chloroform; R_f=1.00, and silica gel, hexane; R_f=0.00 and benzene; R_f=1.00). Red-purple solid. Yield 17%. ^{1}H NMR($CDCl_3$, TMS) δ −2.63 (s. 2H, NH), 0.57–1.00 (m, 48H, CH_3), 1.00–2.33 (m, 192H, CH_2), 3.44–4.17 (m, 32H, OCH_2), 6.47–8.27 (m, 36H, Ph), 8.90 (s, 8H, porphyrin). IR (neat) ν_{max} 3320 (NH), 2930, 2860 (CH_2), 1605, 1580, 1510 (Ph), 1250 cm^{-1} (ROPh).

5,10,15,20-Tetrakis(4,4″-didodecyloxy-*o*-terphenyl)-porphyrin [3; $(C_{12}O)_8$-TTPH$_2$]. The title compound was synthesized from aldehyde **17d** according to the method described above, and purified by column chromatography (silica gel, chloroform; R_f=1.00, alumina, carbon tetrachloride; R_f=0.00, and benzene; R_f=1.00) and recrystallization (hexane, ethyl acetate). Purple solid. Yield 15%. ^{1}H NMR (CCl_4, TMS) δ −2.53 (s, 2H, NH), 0.90 (m, 24H, CH_3), 1.67 (m, 160H, CH_2), 3.77 (m, 12H, OCH_2), 6.40–8.30 (m, 44H, Ph), 8.90 (s, 8H, porphyrin). IR (film) ν_{max} 3320 (NH), 2930, 2860 (CH_2), 1610, 1510 (Ph), 1250 cm^{-1} (ROPh).

5,10,15,20-Tetrakis(3,4,3″,4″-tetradodecyloxy-*o*-terphenyl)-porphyrinatocopper(II) [1-Cu; $(C_{12}O)_{16}$-TTPCu]. Porphyrin **1** (0.12 g, 2.88×10^{-2} mmol) and anhydrous cupric chloride (0.04 g, 0.30 mmol) were dissolved in 30 ml of dry *N,N*-dimethylformamide (DMF) and refluxed for 5 h. The reaction mixture was cooled and separated by filtration. The remaining precipitate was washed by methanol, and purified by column chromatography (alumina, benzene; R_f=1.00) to give 0.11 g

of **1-Cu** as a dark red liquid crystal. Yield 90%. IR (neat) ν_{max} 2930, 2860 (CH_2), 1610, 1580 (Ph), 1250 cm^{-1} (ROPh).

4-Dodecyl-4′-bromobiphenyl (21). A mixture of 4-hydroxy-4′-bromobiphenyl **20** (2.00 g, 8.03 mmol) and potassium hydroxide (0.90 g, 16.0 mmol) in 15 ml of ethanol was refluxed for 1 h. Then a solution of dodecyl bromide (2.10 g, 8.43 mmol) in 5 ml of ethanol was added, and the mixture was further refluxed for 13 h. After cooling to room temperature, the reaction mixture was filtered with suction. The residual precipitate was washed with water and recrystallized from ethanol to afford 1.58 g of **21** as white crystals. m.p. 113 °C. Yield 47%. ^{1}H NMR ($CDCl_3$, TMS) δ 0.87 (m, 3H, CH_3), 1.30 (m, 20H, CH_2), 3.90 (t, J=6.0 Hz, 2H, OCH_2), 6.67–7.50 (m, 8H, Ph). IR (KBr) ν_{max} 2920, 2850 (CH_2), 1600 cm^{-1} (Ph).

4-Formyl-4′-dodecyloxybiphenyl (22). Under a nitrogen atmosphere, 1.6 M butyllithium solution in hexanes (2.6 ml, 4.16 mmol) was added slowly to a solution of **21** (1.50 g, 4.09 mmol) in 30 ml of dry benzene and the mixture was stirred for 30 min at room temperature. *N,N*-Dimethylformamide (DMF; 0.33 g, 4.50 mmol) in 5 ml of benzene was added dropwise, and the reaction mixture was stirred for 2 h at room temperature. The reaction was quenched by dilute hydrochloric acid, and the mixture was extracted with diethyl ether. The organic layer was washed with water, dried over sodium sulfate, and concentrated. After column chromatography (silica gel, benzene; R_f=0.58), 0.49 g of **22** was obtained as a white solid. m.p. 87 °C. Yield 36%. ^{1}H NMR ($CDCl_3$, TMS) δ 0.70 (m, 3H, CH_3), 1.10 (m, 20H, CH_2), 3.73 (t, 2H, OCH_2), 9.58 (s, 1H, CHO). IR (Nujol) ν_{max} 1680 cm^{-1} (CO).

5,15-Bis(3,4,3″,4″-tetradodecyloxy-*o*-terphenyl)porphyrin [4; ($C_{12}O)_8$-BTPH$_2$]. To a solution of aldehyde **17a** (1.43 g, 1.44 mmol) and 2,2′-dipyrrylmethane[44,45] (0.22 g, 1.50 mmol) in 250 ml of dichloromethane, were added seven drops of trifluoroacetic acid, and the solution was stirred for 15 h at room temperature. After *p*-chloranil (1.42 g, 5.78 mmol) was added, the mixture was refluxed for 1 h. The reaction mixture was concentrated, and the residue was purified by column chromatography (alumina, chloroform; R_f=1.00, benzene; R_f=1.00, carbon tetrachloride; R_f=0.00, and silica gel, chloroform; R_f=1.00) and recrystallization from ethyl acetate to give 0.48 g of **4** as a reddish brown solid. Yield 30%. ^{1}H NMR (CCl_4, TMS) δ −3.00 (broad, 2H, NH), 0.87 (m, 24H, CH_3), 1.23 (m, 160H, CH_2), 3.50–4.13 (m, 16H, OCH_2), 6.47–8.40 (m, 18H, Ph), 9.23 (s, 8H, porphyrin), 10.1 (s, 2H, *meso*-H). IR (film) ν_{max} 3300 (NH), 2930, 2860 (CH_2), 1610, 1590 (Ph), 1250 cm^{-1} (ROPh).

5,15-Bis(3,4,3″,4″-tetrahexadecyloxy-*o*-terphenyl)porphyrin [5; ($C_{16}O)_8$-BTPH$_2$]. The title compound was synthesized from aldehyde **17c** by a similar procedure to that described above, and the pure product was obtained by column chromatography (silica gel, chloroform; R_f=1.00, and alumina, chloroform; R_f=1.00) and recrystallization from ethyl acetate and dichloromethane. Brown solid. Yield 57%. ^{1}H NMR (CCl_4, TMS) δ −2.90 (broad, 2H, NH), 0.87 (m, 24H, CH_3), 1.30 (m, 224H, CH_2), 3.50–4.06 (m, 16H, OCH_2), 6.67–8.30 (m, 8H, Ph), 9.10 (s, 8H, porphyrin), 10.0 (s, 2H, *meso*-H). IR (KBr) ν_{max} 3280 (NH), 2930, 2860 (CH_2), 1580 (Ph), 1245 cm^{-1} (ROPh).

5,15-Bis(4,4″-didodecyloxy-*o*-terphenyl)porphyrin [6; ($C_{12}O)_4$-BTPH$_2$]. The title compound was synthesized from aldehyde **17d** by a similar procedure to that described above, and the pure product was obtained by column chromatography (silica gel, chloroform; R_f=1.00, and alumina, chloroform; R_f=1.00) and recrystallization from ethyl acetate and dichloromethane. Reddish brown solid. Yield 39%. ^{1}H NMR (CCl_4, TMS) δ −3.00 (broad, 2H, NH), 0.83 (m, 12H, CH_3), 1.20 (m, 80H, CH_2), 3.46–4.40 (m, 8H, OCH_2), 6.40–8.00 (m, 22H, Ph), 8.83 (s, 8H, porphyrin), 9.77 (s, 2H, *meso*-H). IR (KBr) ν_{max} 3300 (NH), 2930, 2860 (CH_2), 1610 (Ph), 1245 cm^{-1} (ROPh).

5,15-Bis(3,4-didodecyloxyphenyl)porphyrin [7; ($C_{12}O)_4$-BPPH$_2$]. The title compound was synthesized from 3,4-didodecyloxybenzaldehyde **19** by a similar procedure to that described above, and the pure product was obtained by column chromatography (silica gel, benzene; R_f=1.00, and alumina, chloroform; R_f=1.00) and recrystallization from acetone. Purple powder. Yield 33%. ^{1}H NMR (CCl_4, TMS) δ −3.00 (broad, 2H, NH), 0.90 (m, 12H, CH_3), 1.30 (m, 80H, CH_2), 4.13, 4.27 (t+t, 8H, OCH_2), 7.30–7.80 (m, 6H, Ph), 9.07, 9.27 (d+d, 8H, porphyrin), 10.2 (s, 2H, *meso*-H). IR (film) ν_{max} 3285 (NH), 2925, 2855 (CH_2), 1505 (Ph), 1246 cm^{-1} (ROPh).

5,15-Bis(4-dodecyloxybiphenyl)porphyrin [8; ($C_{12}O)_8$-BBPH$_2$]. The title compound was synthesized from 4-formyl-4′-dodecyloxybiphenyl **22** by a similar procedure to that described above. However, because of the low solubility of this compound, the purification was accomplished in the following manner. The reaction mixture was concentrated, and the residue was washed with tetrahydrofuran or dichloromethane and Soxhlet extraction of impurities was performed with acetone–ethyl acetate. The residue was recrystallized from chloroform and dichloromethane to give a dark purple powder. Yield 44%. IR (KBr) ν_{max} 3260 (NH), 2930, 2860 (CH_2), 1600, 1580 (Ph), 1245 cm^{-1} (ROPh).

Notes and references

1 K. Ohta, M. Ando and I. Yamamoto, *J. Porphyrins Phthalocyanines*, in press.
2 M. R. Wasielewski, *Chem. Rev.*, 1992, **92**, 435; J. P. Collman, *Acc. Chem. Res.*, 1977, **10**, 265; D. Gust and T. A. Moore, *Top. Curr. Chem.*, 1991, **159**, 103.
3 B. Morgan and D. Dorphin, *Struct. Bonding*, 1987, **64**, 115.
4 J. L. Sessler and K. A. Burrell, *Top. Curr. Chem.*, 1992, **161**, 177.
5 For example: J. van Esch, M. F. M. Rocks and R. J. M. Nolte, *J. Am. Chem. Soc.*, 1986, **108**, 6093; G. A. Schick, I. C. Schreiman, R. W. Wagner, J. S. Lindsey and D. F. Bocian, *ibid.*, 1989, **111**, 1344; J. T. Groves and R. Newmann, *ibid.*, 1989, **111**, 2900; B. A. Gregg, M. A. Fox and and A. J. Bard, *Tetrahedron*, 1989, **45**, 4704.
6 Y. Suda, K. Shigehara, A. Yamada, H. Matsuda, S. Okada, A. Masaki and H. Nakanishi, *Proc. SPIE-Int. Soc. Opt. Eng.*, 1991, **1560** (*Nonlinear Opt. Prop. Org. Mater.* 4), 75.
7 J. W. Goodby, P. S. Robinson, B.-K. Teo and P. E. Cladis, *Mol. Cryst. Liq. Cryst.*, 1980, **56**, 303.
8 B. A. Gregg, M. A. Fox and A. J. Bard, *J. Chem. Soc., Chem. Commun.*, 1987, 1134; *J. Am. Chem. Soc.*, 1989, **111**, 3024.
9 B. A. Gregg, M. A. Fox and A. J. Bard, *J. Phys. Chem.*, 1990, **94**, 1586.
10 P. G. Schouten, J. M. Warman, M. P. de Haas, M. A. Fox and H.-L. Pan, *Nature*, 1991, **353**, 736.
11 P. Doppelt and S. Huille, *New. J. Chem.*, 1990, **14**, 607.
12 G. Morelli, G. Ricciardi and A. Roviello, *Chem. Phys. Lett.*, 1991, **185**, 468; F. Lelj, G. Morelli, G. Ricciardi, A. Roviello and A. Sirigu, *Liq. Cryst.*, 1992, **12**, 941.
13 Y. Shimizu, M. Miya, A. Nagata, K. Ohta, A. Matsumura, I. Yamamoto and S. Kusabayashi, *Chem. Lett.*, 1991, **25**; Y. Shimizu, M. Miya, A. Nagata, K. Ohta, I. Yamamoto and S. Kusabayashi, *Liq. Cryst.*, 1993, **14**, 795.
14 Y. Shimizu, A. Ishikawa and S. Kusabayashi, *Chem. Lett.*, 1986, 1041.
15 T. Sakaguchi, Y. Shimizu, M. Miya, T. Fukumi, K. Ohta and A. Nagata, *Chem. Lett.*, 1992, 281.
16 R. Ramasseul, P. Maldivi, J.-C. Marchon, M. Taylor and D. Guillon, *Liq. Cryst.*, 1993, **13**, 729.
17 D. W. Bruce, D. A. Dunmur, L. S. Santa and M. A. Wali, *J. Mater. Chem.*, 1992, **2**, 363.

18 For example: C. Piechocki, J. Simon, A. Skoulios, D. Guillon and P. Weber, *J. Am. Chem. Soc*., 1982, **104**, 5245.
19 G. Wenz, *Makromol. Chem. Rapid Commun.*, 1985, **6**, 577.
20 H. Strzelecka, C. Jallabert, M. Veber and J. Malthete, *Mol. Cryst. Liq. Cryst.*, 1988, **156**, 347.
21 G. W. Gray, B. Jones and F. Marson, *J. Chem. Soc.*, 1957, 393.
22 A. D. Adler, F. R. Longo, J. D. Finarelli, J. Goldmacher, J. Assour and L. Korsakoff, *J. Org. Chem.*, 1967, **32**, 476.
23 G. H. Barnett, M. F. Hudson and K. M. Smith, *J. Chem. Soc.*, *Perkin Trans. 1*, 1975, 1401.
24 A. D. Adler, F. R. Longo and V. Váradi, *Inorganic Synthesis*, ed. F. Basolo, McGraw-Hill, New York, 1976, vol. 16, ch. 7, p. 214.
25 J. S. Manka and D. S. Lawrence, *Tetrahedron Lett.*, 1989, **30**, 6989.
26 S. Seki and H. Suga, *Kagaku Sosetsu*, *No. 5, Non-equilibrium states and relaxation processes*, 1974, ch. 9, p. 225.
27 N. Ando, Master Thesis, Shinshu University, Ueda, 1992.
28 M. Ando, Master Thesis, Shinshu University, Ueda, 1993.
29 C. Piechocki, J. Simon, J.-J. André, D. Guillon, P. Petit, A. Skoulios and P. Weber, *Chem. Phys. Lett.*, 1985, **122**, 124.
30 H. R. Kricheldorf and G. Schwarz, *Polymer*, 1990, **31**, 481.
31 B. E. Powell, *J. Cryst. Growth.*, 1973, **18**, 307.
32 G. Lattermann and H. Höcker, *Mol. Cryst. Liq. Cryst.*, 1986, **133**, 245, and references therein.
33 K. Ohta, R. Higashi, M. Ikejima, I. Yamamoto and N. Kobayashi, *J. Mater. Chem*., 1998, **8**, 1979.
34 G. Zerbi, R. Magni, M. Gussoni, K. H. Moritz, A. Bigotto and Dirlikov, *J. Chem. Phys.*, 1981, **75**, 3175.
35 H. L. Casal, H. H. Mantosh, D. G. Cameron and R. G. Snyder, *J. Chem. Phys.*, 1982, **77**, 2825; G. Unger and N. Masic, *J. Phys. Chem.*, 1985, **89**, 1036.
36 C. Almirante, G. Minoni and G. Zerbi, *J. Phys. Chem.*, 1986, **90**, 852.
37 M. Ray-Lafon and T. Hemida, *Mol. Cryst. Liq. Cryst.*, 1990, **178**, 33; W. K. Lee, P.A. Heiney, M. Ohba, J. N. Haseltine and A. B. Smith III, *Liq. Cryst.*, 1990, **8**, 839; W. K. Lee, P. A. Heiney, J. P. McCauley and A. B. Smith III, *Mol. Cryst. Liq. Cryst.*, 1991, **198**, 273.
38 D. Chapman, *Spectrochim. Acta*, 1957, **11**, 609; K. Ohta, M. Yokoyama and H. Mikawa, *Mol. Cryst. Liq. Cryst.*, 1981, **73**, 205.
39 R. G. Snyder, *J. Chem. Phys.*, 1967, **47**, 1316.
40 H. Ema, Master Thesis, Shinshu University, Ueda, 1988.
41 H. Hasebe, Master Thesis, Shinshu University, Ueda, 1991.
42 K. Ohta, T. Watanabe, S. Tanaka, T. Fujimoto, I. Yamamoto, P. Bassoul, N. Kucharczyk and J. Simon, *Liq. Cryst.*, 1991, **10**, 357.
43 T. Watanabe, Master Thesis, Shinshu University, Ueda, 1990.
44 H. Rapoport and C. D. Willson, *J. Am. Chem. Soc.*, 1962, **84**, 630.
45 R. Chong, P. S. Clezy, A. J. Liepa and A. W. Nichol, *Aust. J. Chem.*, 1969, **22**, 229.

Paper 8/05715J